Bull. Chem. Soc. Jpn. Vol. 82, No. 7, 793–805 (2009)

**BCSJ Award Article**

# Synthesis and Properties of Stable 1,2-Bis(metallocenyl)disilenes: Novel d–$\pi$ Conjugated Systems with a Si=Si Double Bond

**Akihiro Yuasa,[1] Takahiro Sasamori,[1] Yoshinobu Hosoi,[2] Yukio Furukawa,[2] and Norihiro Tokitoh*[1]**

[1]Institute for Chemical Research, Kyoto University, Gokasho, Uji, Kyoto 611-0011

[2]Department of Chemistry, School of Science and Engineering, Waseda University,
3-4-1 Okubo, Shinjuku-ku, Tokyo 169-8555

Received December 12, 2008; E-mail: tokitoh@boc.kuicr.kyoto-u.ac.jp

Stable 1,2-bis(metallocenyl)disilenes were synthesized for the first time and were characterized by spectroscopic and X-ray crystallographic analyses. On the basis of cyclic voltammograms, (*E*)-1,2-bis(ferrocenyl)-1,2-bis(2,4,6-triisopropylphenyl)disilene (**1a**) was found to be a stable five-electron redox system with four steps, while (*E*)-1,2-bis(ruthenocenyl)-1,2-bis(2,4,6-triisopropylphenyl)disilene (**1b**) showed four-step redox couples with four electrons. The UV–vis spectra and theoretical calculations for these disilenes suggested that they should be novel d–$\pi$ conjugated systems containing a disilene unit. In addition, chalcogenation reactions of **1a** resulted in the formation of new heterocyclic compounds bearing ferrocenyl units. For example, the first stable 1,2,3,4-dithiadisiletane derivative was obtained by the sulfurization reaction of **1a**.

Organic compounds containing $\pi$-electron systems such as ethylene, benzene, and ketones are of great importance. Especially, extended $\pi$-electron-conjugated systems of organic compounds exhibit lower HOMO–LUMO gaps than those of olefins, showing unique electronic character and possibly applicable to semiconductors, organic electroluminescence, and so on.[1] On the other hand, ferrocene is known to show unique electrochemical properties as a stable redox system.[2] d–$\pi$ Electron-conjugated systems, e.g., multinuclear transition-metal complexes bridged by organic $\pi$-conjugated systems such as phenylene and C=C units, have attracted considerable attention from the viewpoint of their electrochemical properties.[3] Particularly, stable multistep redox systems should be good model systems for the elucidation of the properties of mixed-valence states.[4] Therefore, there has been much interest in the chemistry of ferrocene oligomers bearing a $\pi$-electron spacer, e.g., Fc(Ph)C=C(Ph)Fc,[5] FcN=NFc,[6] and TbtP=PFc (Fc = ferrocenyl),[7] as models of mixed-valence states (Figure 1).

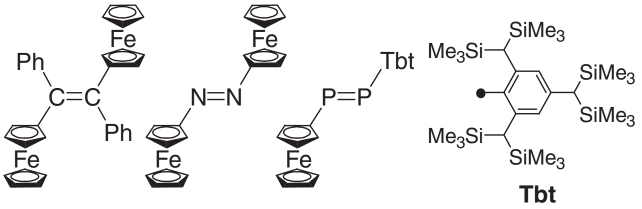

**Figure 1.** d–$\pi$ Conjugated systems.

The first stable disilene as a novel $\pi$-bond system between two silicon atoms was synthesized and isolated by West and his co-workers in 1981.[8] Since disilenes are highly reactive due to the weak $\pi$ bond between silicon atoms, kinetic stabilization should be necessary to isolate and handle disilene derivatives.[9] Since the first isolation of the stable disilene, $Mes_2Si{=}SiMes_2$, numerous examples have been reported for the syntheses and properties of kinetically stabilized silenes,[10] disilenes,[9] and disilynes[11] bearing bulky substituents. Recently, a number of reports on interesting properties of low-coordinated silicon compounds have attracted much attention, e.g., photochemical properties, redox behaviors, and magnetic properties. It has been elucidated that disilenes generally have higher HOMO and lower LUMO levels than those of olefins due to the smaller overlap between the 3p orbitals of Si atoms.[10] Such unique properties of disilenes have prompted many chemists to explore the chemistry of novel extended $\pi$-conjugated systems containing a Si=Si unit from the standpoint of material science. Recently, Bejan and Scheschkewitz[12a] and Tamao et al.[12b] independently reported the synthesis of novel $\pi$-conjugated systems containing Si=Si units. These disilenes have extended $\pi$-conjugated systems with bridged and terminal phenylene or phenyl groups, showing unique photochemical properties (Figure 2).

We have preliminarily reported the synthesis of the first stable 1,2-bis(ferrocenyl)disilene, Tip(Fc)Si=Si(Fc)Tip (**1a**, Tip = 2,4,6-triisopropylphenyl), as a novel stable redox system consisting of a disilene and ferrocenyl units.[13] 1,2-Bis(ferro-

Published on the web July 10, 2009; doi:10.1246/bcsj.82.793

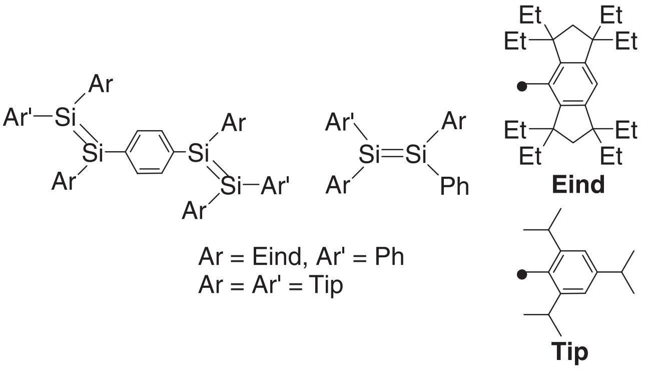

**Figure 2.** Extended $\pi$-conjugated systems with disilene units.

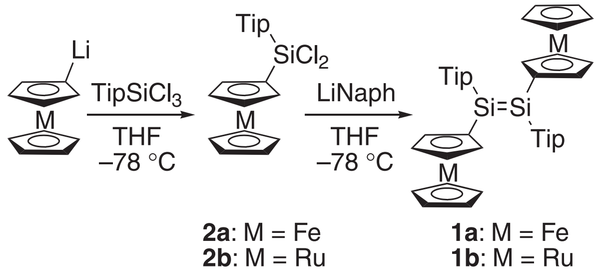

**Scheme 1.** Syntheses of **1a** and **1b**.

cenyl)disilene **1a** exhibits unique redox properties reflecting the stable redox system of ferrocene moieties. On the other hand, ruthenocene, a group 8 metallocene, exhibits higher oxidative potential [half-wave potential ($E_{1/2}$) around +0.5 V vs. FcH/FcH$^+$] than that of ferrocene.[14] Thus, ruthenocene should afford electronic effects different from those shown by ferrocene toward the Si=Si $\pi$-electron system, were it to be introduced to the Si=Si unit as in the case of **1a**. In this paper, we describe the synthesis and properties of ferrocenyl- and ruthenocenyl-substituted disilenes to reveal the effects and role of metallocene units in the novel d–$\pi$ conjugated systems.

## Results and Discussion

In Scheme 1 are shown the synthetic routes for the 1,2-bis(ferrocenyl)disilene **1a** and 1,2-bis(ruthenocenyl)disilene **1b**. Dichlorosilanes **2a** and **2b** bearing a Tip group as steric protection were prepared by reaction of the corresponding metallocenyllithium[15] with TipSiCl$_3$[16] in THF at −78 °C in 49% (**2a**) and 51% (**2b**) yields, respectively. These dichlorosilanes **2a** and **2b** are stable enough to be handled in open air. The structures of **2a** and **2b** were characterized by spectroscopic and X-ray crystallographic analyses (Scheme 1 and Figures 3 and 4). The reduction of **2a** and **2b** with lithium naphthalenide (2.2 equiv) in THF at −78 °C afforded 1,2-bis(metallocenyl)disilenes **1a** (49%) and **1b** (53%) as orange-red and yellow crystals, respectively. After heating the toluene-$d_8$ solution of **1a** in a sealed tube at 90 °C for 10 days, no change was observed in the $^1$H NMR spectra, showing the high thermal stability of **1a** in solution. In addition, **1a** was found to be inert toward photoirradiation (medium pressure Hg lamp, through Pyrex® glass) in $C_6D_6$ solution for 24 h.

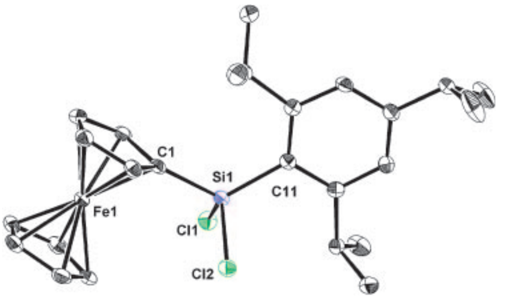

**Figure 3.** ORTEP drawing of **2a** (50% probability). Benezene molecules and hydrogen atoms were omitted for clarity.

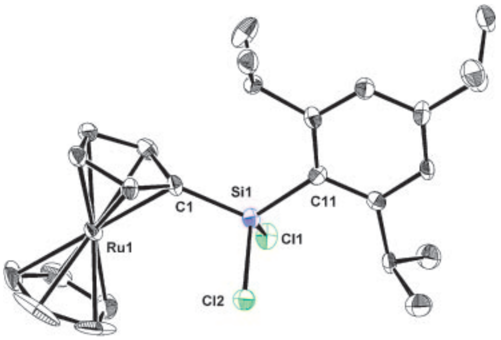

**Figure 4.** ORTEP drawing of **2b** (50% probability). Hydrogen atoms were omitted for clarity.

The $^{29}$Si NMR spectra of **1a** and **1b** in benzene-$d_6$ showed characteristic signals at 72.6 (for **1a**) and 70.6 ppm (for **1b**), which were in the typical range for the sp$^2$ silicon atom of the previously reported disilenes (tetraaryldisilenes, 53–66 ppm; tetraalkyldisilenes, 90–103 ppm).[9d] The $^1$H NMR spectra of **1a** and **1b** in benzene-$d_6$ exhibited a couple of pseudo triplet peaks at 3.80 and 3.98 ppm (for **1a**) and 4.15 and 4.34 ppm (for **1b**), which could be assigned to the protons of the cyclopentadienyl rings. Although the $^1$H NMR spectrum of **1a** suggested that the ferrocenyl and Tip groups should freely rotate around the Si–C bonds without any steric restriction at rt, two doublet signals were observed for the methyl groups [$CH_3$(A) and $CH_3$(B) in Figure 5] of *ortho*-isopropyl groups. That is, these two methyl groups (A) and (B) exhibited two independent doublet signals at 1.514 and 1.529 ppm (at 20 °C), suggesting the trans-bent structure of **1a** in solution as judged by the diastereotopically independent methyl groups. Interestingly, the two methyl groups were observed separately at relatively higher field at elevated temperature (1.496 and 1.514 ppm at 50 °C) as compared with the case at 20 °C, while other signals showed almost no change in the VT-$^1$H NMR spectra (20–50 °C). Accordingly, the trans-bent angle of **1a** should slightly change at 50 °C while maintaining the disilene structure.

Single crystals of **1a** and **1b** suitable for X-ray crystallographic analysis were obtained by recrystallization from THF, and their molecular structures were clearly revealed (Figures 6 and 7 and Table 1). Both disilenes **1a** and **1b** exhibit trans-bent conformations as in the case of the previously reported disilenes, and have a crystallographic center of symmetry at the

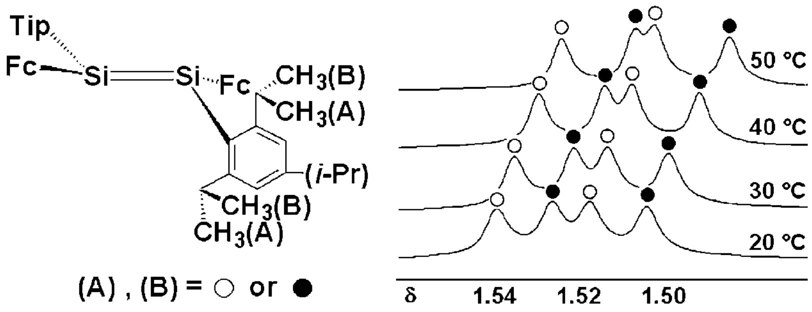

**Figure 5.** VT-$^1$H NMR spectra of **1a** in benzene-$d_6$ (in the methyl-group region).

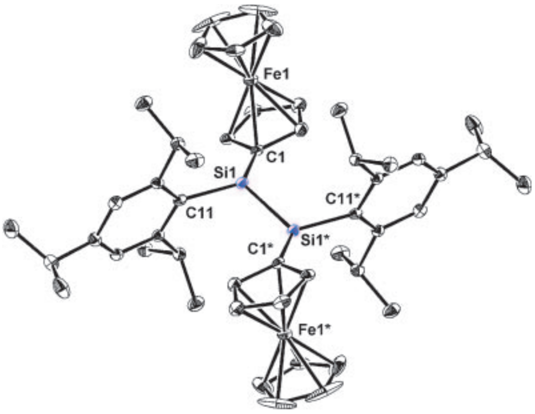

**Figure 6.** ORTEP drawing of **1a** (30% probability). A THF molecule and hydrogen atoms were omitted for clarity.

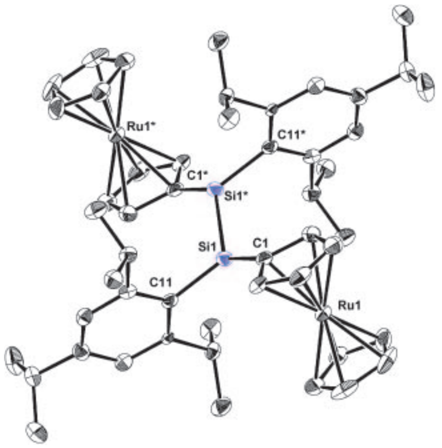

**Figure 7.** ORTEP drawing of **1b** (50% probability). Hydrogen atoms were omitted for clarity.

**Table 1.** Selected Bond Lengths and Angles of **1a** and **1b**

| Bond lengths/Å | | Bond angles/deg | | Trans-bent angles/deg |
|---|---|---|---|---|
| 1,2-Bis(ferrocenyl)disilene **1a** | | | | |
| Si(1)–Si(1)* | 2.1733(15) | C(1)–Si(1)–C(11) | 119.31(12) | 27.9 |
| Si(1)–C(1) | 1.848(3) | C(1)–Si(1)–Si(1)* | 117.94(10) | |
| Si(1)–C(11) | 1.880(3) | C(11)–Si(1)–Si(1)* | 115.08(10) | |
| 1,2-Bis(ruthenocenyl)disilene **1b** | | | | |
| Si(1)–Si(1)* | 2.1851(12) | C(1)–Si(1)–C(11) | 115.98(10) | 32.3 |
| Si(1)–C(1) | 1.845(2) | C(1)–Si(1)–Si(1)* | 116.26(8) | |
| Si(1)–C(11) | 1.887(2) | C(11)–Si(1)–Si(1)* | 116.95(7) | |

center of the Si=Si bond. The trans-bent angles[17] of **1a** and **1b** are 27.9 and 32.3°, respectively, in contrast to the case of $Tip_2Si=SiTip_2$, which was reported to have an almost planar structure. The Si=Si bond lengths of **1a** and **1b** are 2.1733(15) and 2.1851(12) Å, respectively, suggesting the considerable Si=Si double-bond characters of **1a** and **1b** in the solid state as compared with those for the previously reported disilenes (2.14–2.26 Å).[9] The Si–C (*ipso*-metallocenyl) bond lengths of **1a** [1.848(3) Å] and **1b** [1.845(2) Å] are slightly shorter than those of the Si–C (*ipso*-Tip) bonds [1.880(3) Å for **1a**, and 1.887(2) Å for **1b**], suggesting the conjugative interaction between the $\pi$-electrons of the disilene units with those of the Cp rings in both **1a** and **1b**.

Raman spectroscopy may be one of the most useful methods to evaluate the double-bond character of a disilene in the solid state.[9] The Raman spectra of **1a** and **1b** were measured in the solid state with 532 nm excitation in a degassed and sealed tube. In Figure 8 are shown the enlarged partial Raman spectra of **1a** and **1b**, where the most intense signals were observed at 595 and 600 cm$^{-1}$, respectively. Theoretical calculations for **1a** and **1b** showed that the $\nu_{sisi}$ vibrational frequencies should be estimated as 606 and 602 cm$^{-1}$,[18,19] respectively, which were in good agreement with the experimentally observed values. Since the intense Raman shifts corresponding to the Si=Si stretching for the previously reported disilenes bearing carbon-substituents are known to be observed in the range from 500 to 550 cm$^{-1}$,[9,20] the $\nu_{sisi}$ values for **1a** and **1b** are slightly higher than those of the previously reported disilenes. Considering these results, it was found that **1a** and **1b** exhibit enough Si=Si double-bond character in the solid state.

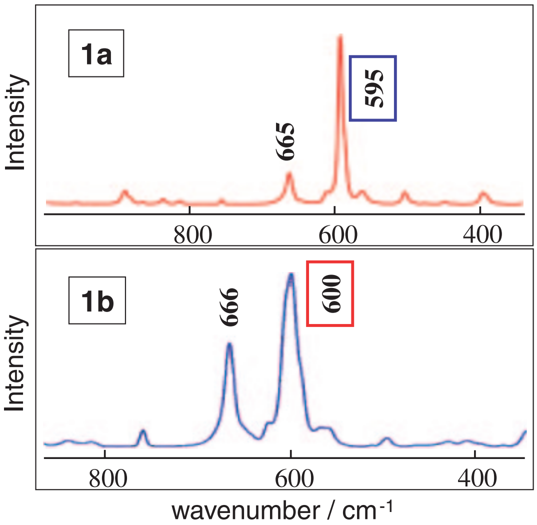

**Figure 8.** Raman spectra of **1a** (top) and **1b** (bottom).

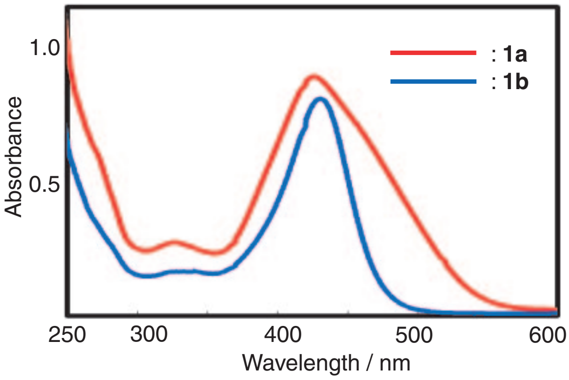

**Figure 9.** UV–vis spectra of **1a** and **1b** in hexane at rt ($3.0 \times 10^{-4}$ mol dm$^{-3}$, 1.0 cm cell).

The UV–vis spectra of **1a** and **1b** in hexane showed two characteristic absorption maxima at 332 ($\varepsilon = 5900$) and 427 nm ($\varepsilon = 24000$) for **1a**, and 340 ($\varepsilon = 5000$) and 430 nm ($\varepsilon = 22000$) for **1b**, respectively, as shown in Figure 9. Tetraaryldisilenes generally show absorption maxima around 400–460 nm assignable to the $\pi$–$\pi^*$ electron transitions of the Si=Si chromophore.[9] TD-DFT calculation for **1a** and **1b** suggested that the observed absorptions at larger wavelength (427 nm for **1a** and 430 nm for **1b**) should be assignable to the mix of electron transitions from Si=Si $\pi$ (HOMO) to Si=Si $\pi^*$ (LUMO) and those from a d-orbital of metallocenyl moiety to the Si=Si $\pi^*$-orbital.[18,19] In addition, the absorption observed at shorter wavelength (332 nm for **1a** and 340 nm for **1b**) should be due to the d–$\pi^*$ electron transitions from metallocenyl moiety to the Si=Si $\pi^*$-orbital. Thus, the two largely observed absorptions should contain several types of d–$\pi^*$ electron transitions to some extent on the basis of the theoretical calculations. The HOMOs and LUMOs of **1a** and **1b** (Figure 10) predominantly consist of the Si=Si $\pi$- and $\pi^*$-orbitals, respectively, while $\pi$- and d-orbitals of ferrocene and ruthenocene units should contribute to the frontier orbitals to some extent. It should be noted that the absorptions for d(M)–$\pi^*$(Si=Si) (M = Fe and Ru) electron transitions of **1a** and **1b** were clearly observed in the visible light region.

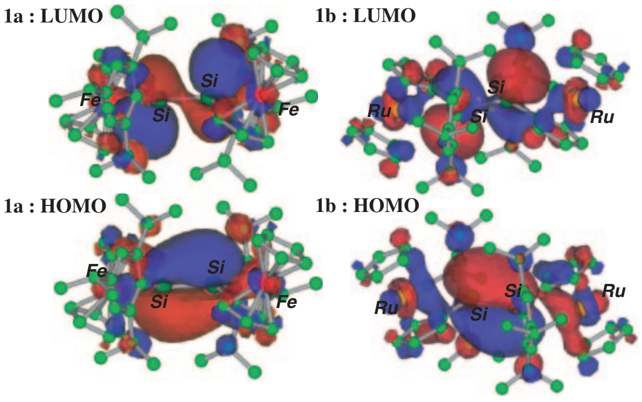

**Figure 10.** Molecular orbitals of **1a** and **1b**.

There have been a number of reports on the electrochemical properties of tetraaryl- or tetrasilyldisilenes.[9,21] The electrochemical properties of disilenes are known to depend on their substituents. For example, tetramesityldisilene showed irreversible waves in oxidation and reduction regions,[21] and Tip$_2$-Si=SiTip$_2$ exhibited irreversible two-electron oxidation and one-electron reduction waves,[21b] while silyl-substituted disilenes show irreversible one-electron oxidation and one-electron reversible and irreversible reduction couples by cyclic voltammetry.[21b] The redox behavior of **1a** and **1b** was revealed by cyclic and differential pulse voltammetries, and their voltammograms are shown in Figures 11 and 12, respectively. The observed redox potentials of **1a** and **1b** are summarized in Tables 2 and 3, respectively. In an *o*-dichlorobenzene solution, two reversible one-electron redox couples corresponding to the stepwise oxidation of the two intramolecular redox centers were observed at $E_{1/2} = +0.05$ and $+0.24$ V (**1a**) and $E_{1/2} = +0.36$ and $+0.56$ V (**1b**) versus FcH/FcH$^+$. Such electrochemical properties of **1a** and **1b** should be most likely interpreted in terms of two conjugated oxidative centers, i.e., two metallocene units, though the HOMOs of **1a** and **1b** seem to dominantly consist of the $\pi$-orbitals of the Si=Si moieties. Furthermore, both two-step oxidative potentials ($E_{1/2}$ values) of **1b** are higher than those of **1a**, probably reflecting the intrinsic nature of metallocenes, i.e., the higher oxidative potential of ruthenocene than that of ferrocene. Thus, the electrochemical properties of metallocenes should be reflected in the unique redox properties of 1,2-bis(metallocenyl)disilenes **1a** and **1b**. The difference between the two oxidation potentials are $\Delta E_{1/2} = 0.19$ (for **1a**) and 0.20 (for **1b**), respectively, which are comparable to that of the corresponding carbon analogue, (*E*)-Ph(Fc)C=C(Fc)Ph (**3**) ($\Delta E_{1/2} = 0.18$ V),[5a] indicating the significant coupling between the two metallocenyl groups of **1a** and **1b** through the Si=Si $\pi$ bond. It should be noted that the two ruthenocenyl moieties of disilene **1b** were found to electrochemically communicate with each other through the Si=Si $\pi$-electrons, in contrast to the case of carbon analogue of **1b**, (*E*)-Me(Rc)C=C(Rc)Me (**4**) (Rc = ruthenocenyl), which is reported to exhibit only one-step oxidation couples with two-electrons, indicating no electronic communication between the two ruthenocenyl moieties bridged by the C=C unit.[22] Thus, the C=C $\pi$-electron system cannot play a role for the d–$\pi$ electron conjugation between the two ruthenocenyl moieties

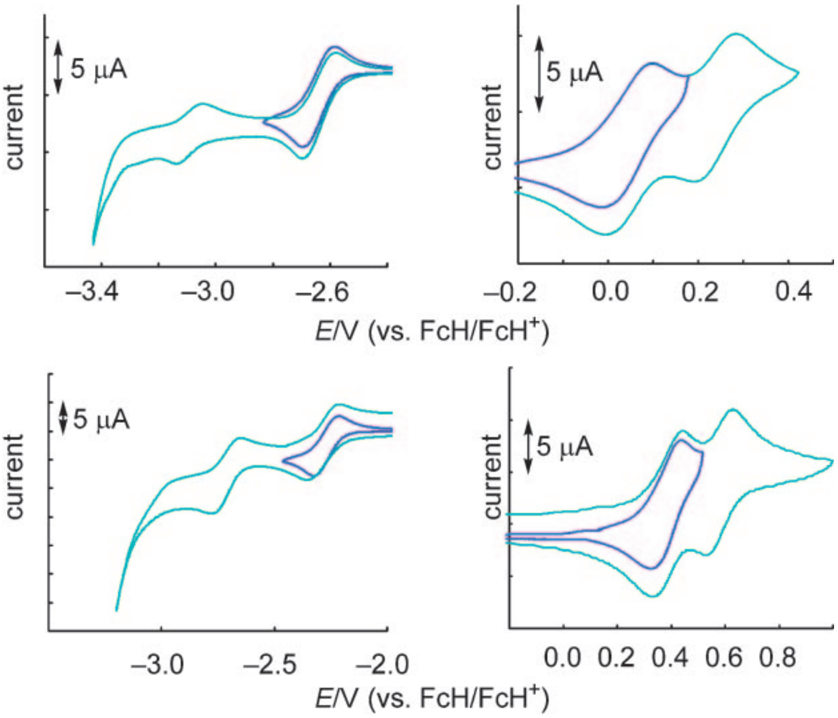

**Figure 11.** Cyclic voltammograms of **1a** (top) and **1b** (bottom). On the left are reductive regions and on the right are oxidative regions.

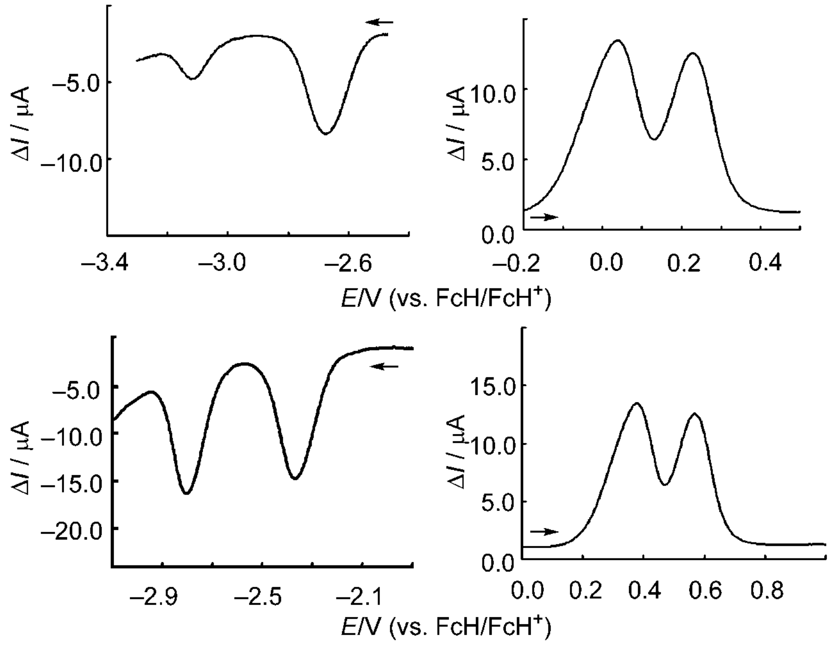

**Figure 12.** Differential pulse voltammograms of **1a** (top) and **1b** (bottom). On the left are reductive regions and on the right are oxidative regions.

probably due to the large difference in size of the orbitals between ruthenocene and ethylene moieties. The large $\pi$-orbital of a disilene unit (Si=Si) can be effectively conjugated with d-orbitals of the ruthenocenyl groups. Therefore, such effective conjugation between the two ruthenocenyl groups through Si=Si $\pi$-electrons seems to be observed in the case of **1b**. On the other hand, cyclic voltammograms of **1a** and **1b** measured in THF solution showed two-step reversible redox couples in the reduction regions at $E_{1/2} = -2.64$ (two electrons) and $-3.09$ V (one electron) for **1a** and $E_{1/2} = -2.38$ (one electron) and $-2.83$ V (one electron) for **1b** (vs. FcH/FcH$^+$), in contrast to the case of **3** and **4**, which were reported to show no evident reduction wave. Such unique properties of the reductions of **1a** and **1b** should be affected by the nature of disilene, since the LUMOs of **1a** and **1b** mainly consist of the $\pi^*$-orbital of their Si=Si unit. While Mes$_2$Si=

**Table 2.** Redox Potentials (V vs. FcH/FcH$^+$) of **1a**

| | | |
|---|---|---|
| Oxidation$^{a)}$ | | |
| $E_{pa}$ | +0.10 | +0.28 |
| $E_{pc}$ | +0.00 | +0.19 |
| $E_{1/2}$ | +0.05 | +0.24 |
| Reduction$^{b)}$ | | |
| $E_{pc}$ | −2.71 | −3.14 |
| $E_{pa}$ | −2.58 | −3.04 |
| $E_{1/2}$ | −2.64 | −3.09 |

a) 0.1 mol dm$^{-3}$ ($n$-Bu)$_4$NB(C$_6$F$_5$)$_4$ in $o$-DCB, $E_{1/2}$ (FcH/FcH$^+$) = +0.34 V vs. Ag/Ag$^+$. b) 0.1 mol dm$^{-3}$ ($n$-Bu)$_4$NPF$_6$ in THF, $E_{1/2}$ (FcH/FcH$^+$) = +0.57 V vs. Ag/Ag$^+$.

**Table 3.** Redox Potentials (V vs. FcH/FcH$^+$) of **1b**

| | | |
|---|---|---|
| Oxidation$^{a)}$ | | |
| $E_{pa}$ | +0.42 | +0.62 |
| $E_{pc}$ | +0.31 | +0.50 |
| $E_{1/2}$ | +0.36 | +0.56 |
| Reduction$^{b)}$ | | |
| $E_{pc}$ | −2.44 | −2.87 |
| $E_{pa}$ | −2.32 | −2.76 |
| $E_{1/2}$ | −2.38 | −2.83 |

a) 0.1 mol dm$^{-3}$ ($n$-Bu)$_4$NB(C$_6$F$_5$)$_4$ in $o$-DCB, $E_{1/2}$ (FcH/FcH$^+$) = +0.37 V vs. Ag/Ag$^+$. b) 0.1 mol dm$^{-3}$ ($n$-Bu)$_4$NPF$_6$ in THF, $E_{1/2}$ (FcH/FcH$^+$) = +0.35 V vs. Ag/Ag$^+$.

SiMes$_2$ was reported to undergo electrochemical reduction irreversibly,[21a] the properties of metallocene units should be reflected in the reversibility of the reduction waves of **1a** and **1b**, that is, the anionic species of **1a** and **1b** should be stabilized by their two metallocene units by effective d–$\pi$ conjugation. Interestingly, the first step of the reduction of **1a** should be two-electron transfer, while that of **1b** should concern only one electron. In addition, both **1a** and **1b** undergo further reduction by one electron after the first step, respectively, i.e., they can be reduced by three (**1a**) and two (**1b**) electrons to afford the corresponding trianion and dianion species. In the case of **1b**, further sweep in the strongly reductive region was unsuccessful under these conditions. Although the difference of the reductive potentials between **1a** and **1b** should be due to the interaction of the metallocene moieties, such phenomena cannot be reasonably explained at present. Thus, it was demonstrated that the metallocenyl groups of **1a** and **1b** should stabilize the corresponding anion and cation species, probably due to the d–$\pi$ electronic conjugative interaction, which should lead to electron delocalization on the extended frontier orbitals of the Si=Si and metallocenyl moieties, in contrast to the case of tetraaryldisilenes such as Mes$_2$Si=SiMes$_2$[21] and Tip$_2$Si=SiTip$_2$,[21b] which show only irreversible reduction in the cyclic voltammogram.

We examined the reactions of **1a** with elemental chalcogens (O$_2$, S$_8$, and Se), since a disilene should be a good precursor for heterocyclic compounds.[23–26] At first, the reactions of **1a** and **1b** with atmospheric oxygen were examined. Exposure of benzene solutions of **1a** and **1b** to air afforded the corresponding four-membered ring compounds, 1,3,2,4-dioxadisiletane **5a** (81%) and **5b** (93%), while Mes$_2$Si=SiMes$_2$ and Tip$_2$Si=SiTip$_2$ were reported to undergo oxidation with ambient oxygen leading to the formation of the corresponding 1,2,3,4-dioxadisiletanes followed by isomerization giving the 1,3,2,4-dioxadisiletane derivatives as final products.[23] Chemical shifts in the $^{29}$Si NMR spectra were observed at 2.50 ppm for **5a** and 12.4 ppm for **5b**, which were within the range of those for the previously reported carbon-substituted 1,3,2,4-dioxadisiletanes (−6.4–13.2 ppm).[23] Next, **1a** was treated with S$_8$ (5 equiv as S) in benzene at rt for 10 min to afford two heterocyclic compounds, thiadisilirane **6** (81%) and 1,2,3,4-dithiadisiletane **7** (13%). In the case of sulfurization reactions of other stable disilenes, RR′Si=SiRR′ (R = R′ = Mes, R = $t$-Bu, R′ = Mes, Tip), with S$_8$ or episulfide, the corresponding thiadisiliranes were obtained as a sole product.[23a,24] Thus, it should be notable that the sulfurization reaction of **1a** gave **7**, which is the first stable 1,2,3,4-dithiadisiletane derivative. In the $^{29}$Si NMR spectra, characteristic signals were observed at −50.8 ppm for **6** and 25.5 ppm for **7**, respectively. The observed $^{29}$Si NMR chemical shift for **6** was within the range of those for the previously reported carbon-substituted thiadisiliranes (−59.0– −28.9 ppm).[24] The observed $\delta_{si}$ value for **7** (25.5 ppm) was reasonably supported by the GIAO-calculations as described below, while that of the imaginary species, 1,3,2,4-dithiadisiletane isomer **8**, was computed as −1.6 ppm at the same calculation level, which is far from the observed value. It the case of tetraaryl-substituted 1,2,3,4-dioxadisiletanes, i.e., oxygen analogues of **7**, the isomerization reaction occurred to give the corresponding 1,3,2,4-dioxadisiletanes at >−30 °C.[23a,23e] However, **7** was stable even at rt for several days. Although one can simply guess that **7** was formed by the further sulfurization of thiadisilirane **6** with S$_8$, the reaction of isolated **6** with an excess of S$_8$ in benzene-$d_6$ at 80 °C resulted in no change even in the presence of NEt$_3$ as an activator of S$_8$.[27] On the contrary, **6** may be formed by the desulfurization of **7** with loss of one S atom. However, **7** was found to be inert toward an excess of PPh$_3$ in benzene-$d_6$ even at 80 °C. That is, it can be concluded that **6** and **7** should be generated by the sulfurization of **1a** directly and the reaction should be kinetically controlled. On the other hand, the reaction of **1a** with elemental selenium (grey Se, 10 equiv) in benzene solution afforded selenadisilirane **9** (95%) exclusively. While the selenization reactions of stable disilenes are known to give the corresponding three-, four-, and six-membered ring heterocyclic compounds containing silicon and selenium atoms depending on the bulkiness and electronic nature of the substituents on the silicon atoms,[25,26,28] Mes$_2$Si=SiMes$_2$ is known to undergo ready selenization leading to the formation of the corresponding selenadisilirane derivative.[25] Thus, the reactivity of **1a** should be very similar to those of Mes$_2$Si=SiMes$_2$. Chemical shifts observed in $^{29}$Si and $^{77}$Se NMR spectra of **9** were observed at −56.4 and −310 ppm, respectively, with $^{29}$Si and $^{77}$Se satellites of $^1J_{SiSe} = 77$ Hz. Those for Mes-substituted selenadisilirane were reported to be $\delta_{si} = -64.8$ and $\delta_{se} = -287$, respectively, with $^{29}$Si and $^{77}$Se satellites of $^1J_{SiSe} = 78$ Hz.[25] As the results of NMR study, it is suggested that **9** and Mes$_2$Si($\mu$-Se)SiMes$_2$ exhibit structural similarities. In contrast to the case of the sulfurization of **1a**, four-membered

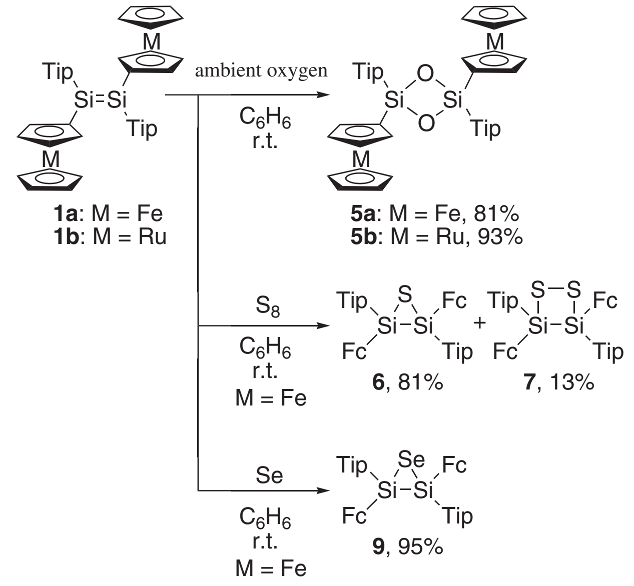

**Scheme 2.** Reactivities of **1a** and **1b**.

ring compounds such as 1,2,3,4-diselenadisiletane were not observed. In some previous reports, deselenization is known to give original low-coordinated species.[29] Attempted deselenization of **9** in a benzene solution by heating or light irradiation with a medium pressure mercury lamp in the presence of $PPh_3$ resulted in no change and no formation of **1a** as judged by $^1H$ NMR spectra (Scheme 2).

We performed theoretical calculations on the relative reaction heat of sulfurization of **1a** leading to the formation of **6**, **7**, and the 1,3,2,4-dithiadisiletane isomer **8**, where the reaction heats were estimated as −55.8 (for **6**), −51.2 (for **7**), and $-101.7\,\mathrm{kcal\,mol^{-1}}$ ($1\,\mathrm{kcal\,mol^{-1}} = 4.184\,\mathrm{kJ\,mol^{-1}}$) (for **8**) (Figure 13).[19,30] 1,3,2,4-Dithiadisiletane **8** should be the thermodynamic product in the reaction of **1a** with $S_8$, while the obtained products, **6** and **7**, should be the kinetic products. These results are not likely to be specific to ferrocenyl- and Tip-substituted disilene **1a** but general for tetraaryldisilenes, since theoretical calculations for the reactions of $Ph_2Si{=}SiPh_2$ with $S_8$ leading to the formation of the corresponding thiadisilirane **10**, 1,2,3,4,- and 1,3,2,4-dithiadisiletanes **11** and **12** showed results similar to those for **1a** as shown in Figure 14.[19,30] The experimental observation that thermal transformation of **7** into 1,3,2,4-dithiadisiletane fails even at 140 °C is most likely interpreted in terms of the severe steric congestion around the two sulfur atoms of **7** due to the ferrocenyl and Tip groups.

Single crystals of **5a**, **5b**, **6**, **7**, and **9** suitable for X-ray diffraction study were obtained by recrystallization from hexane (for **5a**, **5b**, **6**, and **7**) and toluene (for **9**) (Figures 15–19). The Si–O bond lengths of **5a** and **5b** were ca. 1.67 Å, which were within the bond lengths between silicon and oxygen of previously reported 1,3,2,4-dioxadisiletanes (1.66–1.72 Å).[23] Sums of the internal angles of the central four-membered ring systems of **5a** and **5b** were ca. 360° in both cases, showing the planar structures of the Si–O–Si–O squares, as in the cases of $Mes_2Si(\mu\text{-}O)_2SiMes_2$[23b] and $Tip_2Si(\mu\text{-}O)_2SiTip_2$.[23d]

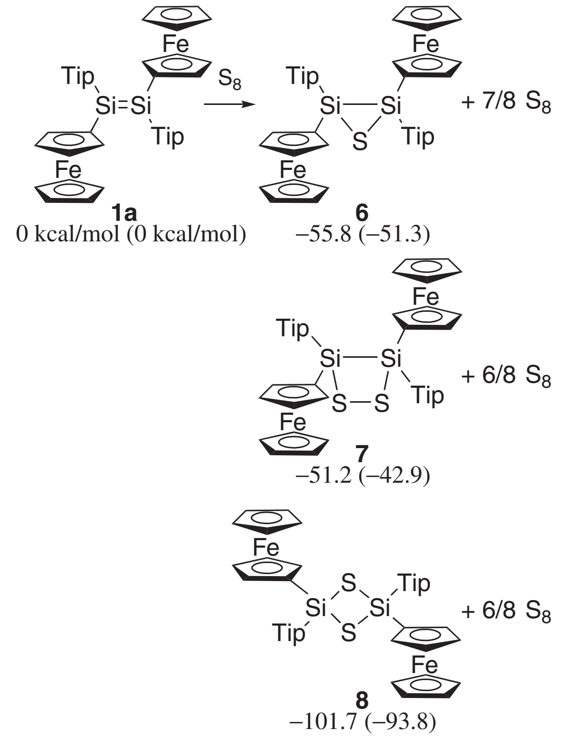

**Figure 13.** Theoretical calculations for the sulfurization of **1a** with elemental sulfur. SCF energies in $\mathrm{kcal\,mol^{-1}}$ (free energy, 0 atm, 25 °C) are shown in parenthetical reference.[30]

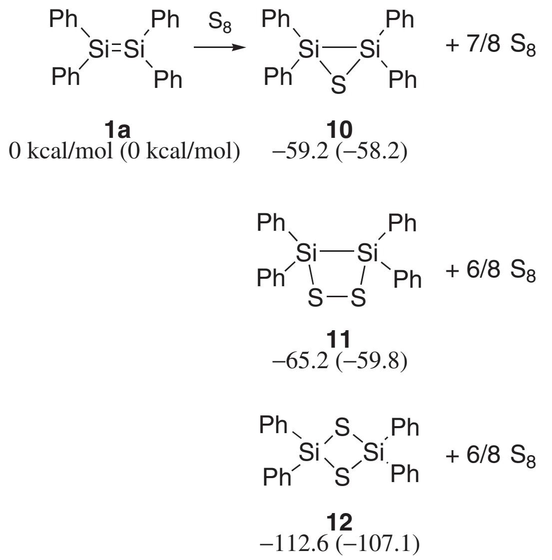

**Figure 14.** Theoretical calculations for the sulfurization of $Ph_2Si{=}SiPh_2$ with elemental sulfur. SCF energies in $\mathrm{kcal\,mol^{-1}}$ (free energy, 0 atm, 25 °C) are shown in parenthetical reference.[30]

On the other hand, the sum of the internal angles of the Si–S–S–Si square of 1,2,3,4-dithiadisiletane **7** was found to be ca. 338°, showing its folded-square structure as in the case of Si–O–O–Si and Sn–S–S–Sn squares of previously reported 1,2,3,4-dioxadisiletane[23e] and 1,2,3,4-dithiadistannetane[31] derivatives.

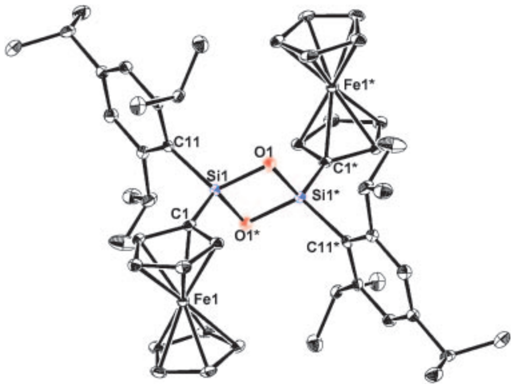

**Figure 15.** ORTEP drawing of **5a** (50% probability). Hydrogen atoms were omitted for clarity.

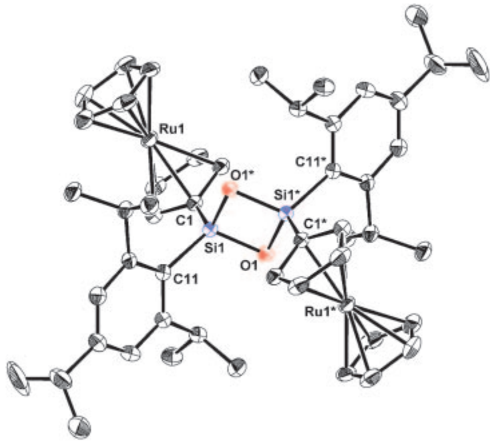

**Figure 16.** ORTEP drawing of **5b** (30% probability). Hydrogen atoms were omitted for clarity.

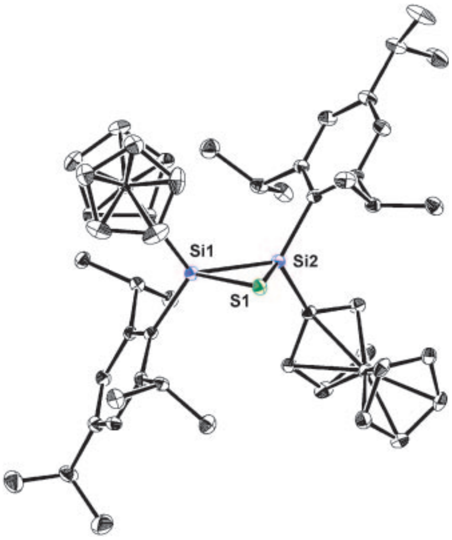

**Figure 17.** ORTEP drawing of **6** (30% probability). Hexane molecule and hydrogen atoms were omitted for clarity.

The structures of the obtained chalcogenadisiliranes, **6** and **9**, were similar to each other with a Si–Si–Ch (Ch = S and Se) isosceles triangle. The Si–Si bond lengths of **6** and **9** are 2.2782(13) and 2.2876(12) Å, respectively, which are slightly shorter than the typical Si–Si single bond lengths (2.33–2.37 Å)[32] and that of **7** [2.3685(12) Å]. In previous reports, tetramesitylchalcogenadisiliranes were found to have slightly shorter Si–Si bonds, which can be most likely interpreted in terms of the $\pi$-complex character of chalcogenadisilirane derivatives.[24,25] Thus, **6** and **9** were thought to exhibit considerable $\pi$-complex character of chalcogenadisiliranes (Table 4).

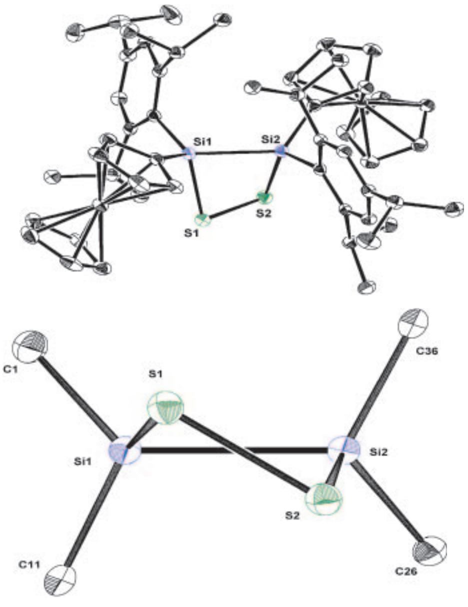

**Figure 18.** ORTEP drawing of **7** [50% probability, side view (top) and top view (bottom)]. Hydrogen atoms were omitted for clarity.

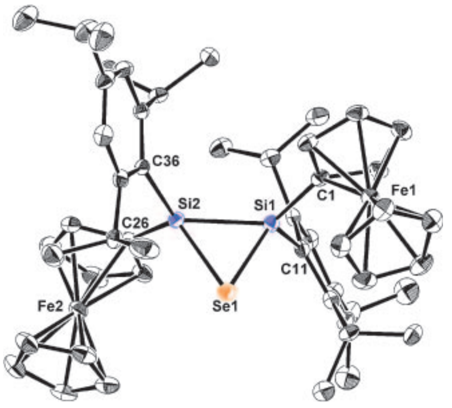

**Figure 19.** ORTEP drawing of **9** (50% probability). A toluene molecule and hydrogen atoms were omitted for clarity.

Theoretical calculations for **5a**, **5b**, **6**, **7**, and **9** were performed.[19,30] In all cases, the optimized structural parameters are in good agreement with those experimentally observed. On the other hand, the $\delta_{\mathrm{Si}}$ chemical shifts were computed as 1.4 for **5a**, −2.45 for **5b**, −56.9 for **6**, 28.2 and 26.5 for **7**, and −53.4 for **9** by GIAO calculations,[19,30] the values of which are reasonably in good agreement with the corresponding observed chemical shifts, supporting their molecular structures in solution. In addition, $\delta_{\mathrm{Si}}$ value of 1,3,2,4-dithiadisiletane **8** was computed as −1.6 ppm, showing a large difference from those observed and calculated for 1,2,3,4-dithiadisiletane **7**. In

**Table 4.** Selected Bond Lengths and Angles of Chalcogenation Products

| Bond lengths/Å | | Bond angles/deg | |
|---|---|---|---|
| Ferrocenyldioxadisiletane **5a** | | | |
| Si(1)–Si(1)* | 2.4111(9) | O(1)–Si(1)–O(1)* | 88.48(6) |
| Si(1)–O(1) | 1.6855(12) | Si(1)–O(1)–Si(1)* | 91.52(6) |
| Si(1)–O(1)* | 1.6798(12) | O(1)–Si(1)–Si(1)* | 44.14(4) |
| | | O(1)*–Si(1)–Si(1)* | 44.33(4) |
| Ruthenocenyldioxadisiletane **5b** | | | |
| Si(1)–Si(1)* | 2.409(2) | O(1)–Si(1)–O(1)* | 88.55(13) |
| Si(1)–O(1) | 1.689(3) | Si(1)–O(1)–Si(1)* | 91.45(13) |
| Si(1)–O(1)* | 1.675(3) | O(1)–Si(1)–Si(1)* | 44.04(10) |
| | | O(1)*–Si(1)–Si(1)* | 44.51(9) |
| Thiadisilirane **6** | | | |
| Si(1)–Si(2) | 2.2782(13) | Si(1)–Si(2)–S(1) | 63.30(4) |
| Si(1)–S(1) | 2.1717(13) | Si(1)–S(1)–S(2) | 58.38(4) |
| Si(2)–S(1) | 2.1702(14) | S(1)–Si(1)–Si(2) | 58.32(4) |
| Dithiadisiletane **7** | | | |
| Si(1)–Si(2) | 2.3685(12) | Si(1)–Si(2)–S(2) | 82.19(4) |
| Si(1)–S(1) | 2.1875(12) | Si(2)–Si(1)–S(1) | 80.56(4) |
| Si(2)–S(2) | 2.1782(12) | Si(1)–S(1)–S(2) | 88.25(4) |
| S(1)–S(2) | 2.1095(12) | Si(2)–S(2)–S(1) | 86.88(5) |
| Selenadisilirane **8** | | | |
| Si(1)–Si(2) | 2.2876(12) | Si(1)–Si(2)–Se(1) | 60.51(3) |
| Si(1)–Se(1) | 2.3134(9) | Si(1)–Se(1)–Si(2) | 59.40(3) |
| Si(2)–Se(1) | 2.3035(8) | Se(1)–Si(1)–Si(2) | 60.08(3) |

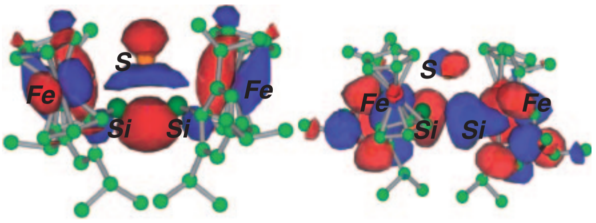

**Figure 20.** HOMO (left) and LUMO (right) orbitals of **6**.

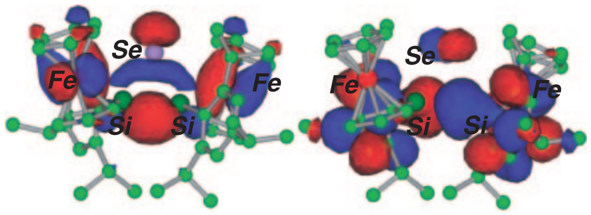

**Figure 21.** HOMO (left) and LUMO (right) orbitals of **9**.

the case of **9**, the calculated $\delta_{\mathrm{se}}$ value of −321 is similar to that observed for **9** in $C_6D_6$ solution. Thus, the molecular structures of the newly obtained chalcogenacycles were reasonably supported by the results of theoretical calculations. Here, the calculated HOMO of chalcogenadisiliranes **6** and **9** should be notable, since it should be indicative of their $\pi$-complex character (Figures 20 and 21). As expected, both of the calculated HOMOs of **6** and **9** were computed to dominantly consist of $\pi$-orbitals of the Si=Si moiety and $\pi$-orbitals of the chalcogen atom (S for **7** and Se for **9**), indicating the $\pi$-complex character (Scheme 3).[24,25,33]

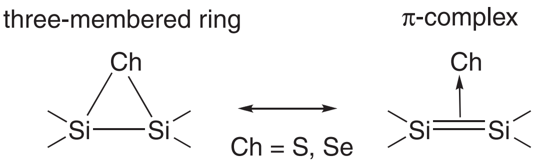

**Scheme 3.** Resonance structures of chalcogenadisilirane.

The reactivity of **1a** should be predominantly characterized by the Si=Si unit rather than the ferrocenyl unit. The redox behavior of chalcogenacyclic compounds with ferrocenyl and ruthenocenyl groups will be clarified in the future.

## Conclusion

We have successfully synthesized the first stable 1,2-bis(metallocenyl)disilenes as novel d–$\pi$ conjugated systems with a Si=Si double bond. They are the first disilenes with functionality afforded by metallocenyl units. They showed multi-step reversible redox couples in contrast to 1,2-bis(metallocenyl)ethenes and tetraaryldisilenes. The d-orbital of the metal at the metallocenyl center and the $\pi$-orbital of the disilene units appear to be conjugated via the cyclopentadienyl rings on the basis of spectroscopic analyses. The d–$\pi$ electron transitions were observed by UV–vis spectra. In addition, we have succeeded in the synthesis of new ferrocenyl-substituted heterosilacyclic compounds by the chalcogenation reaction of **1a**. Significantly, the first 1,2,3,4-dithiadisiletane was obtained as a stable compound.

## Experimental

**General Comments.** All experiments were performed under an argon atmosphere unless otherwise noted. All solvents were purified by standard methods and then dried by using an Ultimate Solvent System (Glass Contour Co.).[34] Solvents used in spectroscopy (benzene-$d_6$) were dried by using a potassium mirror and *o*-dichlorobenzene was distilled from $CaH_2$. Preparative gel permeation liquid chromatography (GPLC) was performed on an LC-908 or LC-918 apparatus equipped with JAI-gel 1H and 2H columns (Japan Analytical Industry Co., Ltd.) with toluene as an eluent. $^1$H NMR (400 or 300 MHz) and $^{13}$C NMR (100 or 75 MHz) spectra were measured in $C_6D_6$ with a JEOL AL-400 or -300 spectrometer using signals for $C_6HD_5$ ($\delta$ 7.15), $C_6D_5CH_3$ ($\delta$ 2.10), and $C_6D_6$ ($\delta$ 128.0) as internal standards for $^1$H and $^{13}$C NMR spectra, respectively. $^{29}$Si NMR (59 MHz) spectra were measured in $C_6D_6$ with a JEOL AL-300 spectrometer using the signal for $SiMe_4$ ($\delta$ 0) in $C_6D_6$ as an external standard. $^{77}$Se NMR (76 or 57 MHz) spectra were measured in $C_6D_6$ with a JEOL AL-400 or -300 spectrometer using $Ph_2Se_2$ in $C_6D_6$ ($\delta$ 460) as an external standard. High-resolution mass spectral data were obtained on a JEOL JMS-700 spectrometer (FAB) or a Bruker microTOF (APPI-TOF). Electronic spectra were recorded on a JASCO V-570 UV–vis spectrometer. Raman spectra were measured on a Raman spectrometer consisting of a Spex 1877 Triplemate and an EG&G PARC 1421 intensified photodiode array detector. An NEC GLG 108 He-Ne laser was used for Raman excitation. The electrochemical experiments were carried out with an ALS 602A electrochemical analyzer using a glassy carbon disk working electrode, a Pt wire counter electrode, and Ag/0.01 M $AgNO_3$ reference electrode. The measurements were carried out in *o*-dichlorobenzene or THF solution containing 0.1 M $(n\text{-Bu})_4NB(C_6F_5)_4$ or $(n\text{-Bu})_4NPF_6$ as a supporting electrolyte with scan rates of 10 mV s$^{-1}$ in a glovebox filled with argon at ambient temperature. All melting points were determined on a Yanaco micro melting point apparatus and are uncorrected. Elemental analyses were performed by the Microanalytical Laboratory of the Institute for Chemical Research, Kyoto University. All calculations were conducted using the Gaussian 03 series of electronic structure programs.[35] FcI[15] and $TipSiCl_3$[16] were prepared according to reported procedures. It was confirmed by frequency calculations that the optimized structures have minimum energies. Computation time was provided by the Supercomputer Laboratory, Institute for Chemical Research, Kyoto University.

**Synthesis of Dichloro(ferrocenyl)(2,4,6-triisopropylphenyl)silane (2a).** To a THF solution (30 mL) of FcI (914 mg, 2.93 mmol) was added a pentane solution of *t*-BuLi (1.58 mol dm$^{-3}$, 3.91 mL, 6.15 mmol) at −78 °C. After stirring the solution for 30 min at the same temperature, the reaction mixture was warmed to room temperature. To the reaction mixture containing the resulting FcLi was added a THF solution (60 mL) of $TipSiCl_3$ (1.00 g, 2.93 mmol) at −78 °C. After stirring for 30 min at the same temperature, the reaction mixture was warmed to room temperature. After removal of the solvent, the reaction mixture was filtered through Celite® with hexane, and the solvent of the filtrate was removed under reduced pressure. The residue was subjected to GPLC (toluene) to give $TipFcSiCl_2$ (**2a**, 704 mg, 1.44 mmol, 49%). **2a**; orange crystals; mp 162.6–164.0 °C; $^1$H NMR (300 MHz, rt, $C_6D_6$): $\delta$ 1.14 (d, 6H, *p*-*i*Pr-Me, $^3J_{HH} = 6.6$ Hz), 1.22 (d, 12H, *o*-*i*Pr-Me, $^3J_{HH} = 6.6$ Hz), 2.69 (sept, 1H, *p*-*i*Pr-CH, $^3J_{HH} = 6.6$ Hz), 3.91 (sept, 2H, *o*-*i*Pr-CH, $^3J_{HH} = 6.6$ Hz), 4.20 (pseudo-t, 2H), 4.23 (s, 5H, Cp), 4.41 (pseudo-t, 2H), 7.12 (s, 2H, Ar-H); $^{13}$C NMR (75 MHz, rt, $C_6D_6$): $\delta$ 23.82 (q), 25.09 (q), 33.06 (d), 34.76 (d), 70.48 (d), 72.25 (d), 74.61 (d), 74.74 (s), 122.51 (d), 128.09 (s), 152.62 (s), 156.39 (s); $^{29}$Si NMR (59 MHz, rt, $C_6D_6$): $\delta$ 9.53. HRMS (FAB) *m*/*z*: Calcd for $C_{25}H_{32}{}^{35}Cl_2{}^{56}FeSi$ 486.1001 $[M]^+$. Found 486.1017 $[M]^+$. Anal. Calcd for $C_{25}H_{32}Cl_2FeSi$: C, 61.61; H, 6.62; Cl, 14.55%. Found: C, 61.51; H, 6.68; Cl, 14.28%.

**Synthesis of Dichloro(ruthenocenyl)(2,4,6-triisopropylphenyl)silane (2b).** To a THF solution (30 mL) of ruthenocene (342 mg, 1.48 mmol) was added a pentane solution of *t*-BuLi (1.58 mol dm$^{-3}$, 1.13 mL, 1.77 mmol) at −78 °C. After stirring the solution for 30 min at the same temperature, the reaction mixture was warmed to room temperature. To the reaction mixture containing the resulting RcLi was added a THF solution (60 mL) of $TipSiCl_3$ (500 mg, 1.48 mmol) at −78 °C. After stirring for 30 min at the same temperature, the reaction mixture was warmed to room temperature. After removal of the solvent, the reaction mixture was filtered through Celite® with hexane, and the solvent of the filtrate was removed under reduced pressure. The residue was subjected to GPLC (toluene) to give $TipRcSiCl_2$ (**2b**, 401 mg, 0.752 mmol, 51%). **2b**; colorless crystals; mp 150.0–151.6 °C; $^1$H NMR (300 MHz, rt, $C_6D_6$): $\delta$ 1.16 (d, 6H, *p*-*i*Pr-Me, $^3J_{HH} = 6.6$ Hz), 1.26 (d, 12H, *o*-*i*Pr-Me, $^3J_{HH} = 6.6$ Hz), 2.71 (sept, 1H, *p*-*i*Pr-CH, $^3J_{HH} = 6.6$ Hz), 4.03 (sept, 2H, *o*-*i*Pr-CH, $^3J_{HH} = 6.6$ Hz), 4.58 (pseudo-t, 2H), 4.62 (s, 5H, Cp), 4.80 (pseudo-t, 2H), 7.12 (s, 2H, Ar-H); $^{13}$C NMR (75 MHz, rt, $C_6D_6$): $\delta$ 23.83 (q), 25.41 (q), 33.32 (d), 34.65 (d), 72.98 (d), 73.82 (d), 76.04 (d), 78.80 (s), 122.52 (d), 127.90 (s), 152.62 (s), 156.46 (s); $^{29}$Si NMR (59 MHz, rt, $C_6D_6$): $\delta$ 7.59. HRMS (FAB) *m*/*z*: Calcd for $C_{25}H_{32}{}^{35}Cl_2{}^{102}RuSi$ 532.0694 $[M]^+$. Found 532.0692 $[M]^+$. Anal. Calcd for $C_{25}H_{32}Cl_2RuSi$: C, 56.38; H, 6.06; Cl, 13.31%. Found: C, 56.53; H, 6.14; Cl, 13.01%.

**Synthesis of (*E*)-1,2-Bis(ferrocenyl)-1,2-bis(2,4,6-triisopropylphenyl)disilene (1a).** To a THF solution (15 mL) of **2a** (200 mg, 0.410 mmol) was added a THF solution of lithium naphthalenide (0.300 mol dm$^{-3}$, 3.00 mL, 0.900 mmol) at −78 °C. After stirring for 30 min at the same temperature, the reaction mixture was warmed to room temperature. After the removal of solvent, the mixture was extracted with hexane several times and then filtered with Celite®. The solvent of the filtrate was removed under reduced pressure to afford Tip(Fc)Si=Si(Fc)Tip (**1a**, 84.3 mg, 0.101 mmol, 49%). **1a**; red crystals; mp 160.4–163.3 °C; $^1$H NMR (300 MHz, rt, $C_6D_6$): $\delta$ 1.28 (d, 12H, *p*-*i*Pr-Me, $^3J_{HH} = 6.6$ Hz), 1.51 (d, 12H, *o*-*i*Pr-Me, $^3J_{HH} = 6.6$ Hz), 1.53 (d, 12H, *o*-*i*Pr-Me, $^3J_{HH} = 6.6$ Hz), 2.89 (sept, 2H, *p*-*i*Pr-CH, $^3J_{HH} = 6.6$ Hz), 3.80 (pseudo-t, 4H), 3.96 (s, 10H, Cp), 3.98 (pseudo-t, 4H), 4.29 (sept, 4H, *o*-*i*Pr-CH, $^3J_{HH} = 6.6$ Hz), 7.34 (s, 4H, Ar-H); $^{13}$C NMR (75 MHz, rt, $C_6D_6$): $\delta$ 24.19 (q), 24.33 (q), 26.39 (q), 34.87 (d), 38.73 (d), 68.77 (s), 69.12 (d), 71.27 (d), 73.42 (d), 121.40 (d), 130.71 (s), 151.85 (s), 156.61 (s); $^{29}$Si NMR (59 MHz, rt, $C_6D_6$): $\delta$ 72.6. UV–vis (hexane) $\lambda_{max}$/nm ($\varepsilon$) = 332 ($5.9 \times 10^3$), 427 ($2.4 \times 10^4$). HRMS (APPI-TOF) *m*/*z* Calcd for $C_{50}H_{65}{}^{56}Fe_2Si_2$ 833.3321 $[M + H]^+$. Found 833.3371 $[M + H]^+$. Anal. Calcd for $C_{50}H_{64}Fe_2Si_2$: C, 72.10; H, 7.74%. Found: C, 72.35; H, 7.98%.

**Synthesis of (*E*)-1,2-Bis(ruthenocenyl)-1,2-bis(2,4,6-triisopropylphenyl)disilene (1b).** To a THF solution (5 mL) of **2b** (100 mg, 0.188 mmol) was added a THF solution of lithium naphthalenide (0.300 mol dm$^{-3}$, 1.38 mL, 0.414 mmol) at −78 °C. After stirring for 30 min at the same temperature, the reaction mixture was warmed to room temperature. After the removal of solvent, the mixture was extracted with hexane several times and then filtered with Celite®. The solvent of the filtrate was removed under reduced pressure to afford Tip(Rc)Si=Si(Rc)Tip (**1b**, 92.0 mg, 0.100 mmol, 53%). **1b**; light yellow crystals; mp 180.2–183.0 °C; $^1$H NMR (300 MHz, rt, $C_6D_6$): $\delta$ 1.25 (d, 12H, *p*-*i*Pr-Me, $^3J_{HH} = 6.9$ Hz), 1.50 (d, 12H, *o*-*i*Pr-Me, $^3J_{HH} = 6.6$ Hz), 1.52 (d, 12H, *o*-*i*Pr-Me, $^3J_{HH} = 6.6$ Hz), 2.85 (sept, 2H, *o*-*i*Pr-CH, $^3J_{HH} = 6.9$ Hz), 4.15 (pseudo-t, 4H), 4.21 (sept, 4H, *o*-*i*Pr-CH, $^3J_{HH} = 6.6$ Hz), 4.34 (pseudo-t, 4H), 4.40 (s, 10H, Cp), 7.30 (s, 4H, Ar-H); $^{13}$C NMR (75 MHz, rt, $C_6D_6$): $\delta$ 24.16 (q), 24.30 (q), 26.49 (q), 34.84 (d), 38.75 (d), 71.27 (s), 71.42 (d), 72.78 (d), 75.48 (d), 121.27 (d), 130.66 (s), 151.74 (s), 156.49 (s); $^{29}$Si NMR (59 MHz, rt, $C_6D_6$): $\delta$ 70.6. UV–vis (hexane) $\lambda_{max}$/nm ($\varepsilon$) = 340 ($5.0 \times 10^3$), 430 ($2.2 \times 10^4$). HRMS (APPI-TOF) *m*/*z* Calcd for $C_{50}H_{65}{}^{102}Ru_2Si_2$ 925.2730 $[M + H]^+$. Found 925.2709 $[M + H]^+$. Anal. Calcd for $C_{50}H_{64}Ru_2Si_2$: C, 65.04; H, 6.99%. Found: C, 64.83; H, 7.15%.

**Irradiation of a Benzene Solution of 1a.** A benzene-$d_6$ solution (4 mL) of **1a** (5.0 mg, 6.0 µmol) in a sealed tube was irradiated with a medium pressure mercury lamp for 1 h through a Pyrex® NMR tube. No change was observed as judged by $^1$H NMR spectra.

**Reaction of (*E*)-1,2-Bis(ferrocenyl)-1,2-bis(2,4,6-triisopropylphenyl)disilene (1a) with Oxygen.** A benzene solution (5 mL) of **1a** (20.0 mg, 24.0 µmol) was exposed to open air at room temperature. The solution then turned colorless. After removal of solvent, the reaction mixture was separated by GPLC to afford corresponding 1,3,2,4-dioxadisiletane, Tip(Fc)Si($\mu$-O)$_2$Si(Fc)Tip (**5a**, 16.9 mg, 19.5 µmol, 81%). **5a**; yellow crystals; sublimation point 265.2–266.4 °C; $^{1}$H NMR (300 MHz, rt, $C_6D_6$): $\delta$ 1.23 (d, 12H, *p-i*Pr-Me, $^{3}J_{HH} = 6.6$ Hz), 1.38 (d, 12H, *o-i*Pr-Me, $^{3}J_{HH} = 6.6$ Hz), 1.64 (d, 12H, *o-i*Pr-Me, $^{3}J_{HH} = 6.6$ Hz), 2.82 (sept, 2H, *p-i*Pr-CH, $^{3}J_{HH} = 6.6$ Hz), 4.02 (ABq, 4H, Cp, $^{3}J_{HH} = 9.6$ Hz), 4.03 (sept, 4H, *o-i*Pr-CH, $^{3}J_{HH} = 6.6$ Hz), 4.10 (s, 10H, Cp), 4.11 (ABq, 4H, Cp, $^{3}J_{HH} = 9.6$ Hz), 7.41 (s, 4H, Ar-H); $^{13}$C NMR (75 MHz, rt, $C_6D_6$): $\delta$ 24.07 (q), 25.30 (q), 25.83 (q), 34.60 (d), 34.80 (d), 68.81 (s), 68.97 (d), 71.81 (d), 74.55 (d), 121.39 (d), 128.53 (s), 151.98 (s), 156.39 (s); $^{29}$Si NMR (59 MHz, rt, $C_6D_6$): $\delta$ 2.50. HRMS (FAB) *m/z* Calcd for $C_{50}H_{64}O_2{}^{56}Fe_2Si_2$ 864.3147 $[M]^+$. Found 864.3140 $[M]^+$. Anal. Calcd for $C_{50}H_{64}O_2Fe_2Si_2$: C, 69.43; H, 7.46%. Found: C, 69.29; H, 7.41%.

**Reaction of (*E*)-1,2-Bis(ruthenocenyl)-1,2-bis(2,4,6-triisopropylphenyl)disilene (1b) with Oxygen.** A benzene solution (5 mL) of **1b** (20.0 mg, 21.6 µmol) was exposed to open air at room temperature. The solution then turned colorless in next to no time. After removal of solvent, the reaction mixture was separated by GPLC to afford corresponding 1,3,2,4-dioxadisiletane, Tip(Rc)-Si($\mu$-O)$_2$Si(Rc)Tip (**5b**, 19.2 mg, 20.1 µmol, 93%). **5b**; colorless crystals; sublimation point 266.1–270.4 °C; $^{1}$H NMR (300 MHz, rt, $C_6D_6$): $\delta$ 1.20 (d, 12H, *p-i*Pr-Me, $^{3}J_{HH} = 6.6$ Hz), 1.39 (d, 12H, *o-i*Pr-Me, $^{3}J_{HH} = 6.6$ Hz), 1.62 (d, 12H, *o-i*Pr-Me, $^{3}J_{HH} = 6.6$ Hz), 2.80 (sept, 2H, *p-i*Pr-CH, $^{3}J_{HH} = 6.6$ Hz), 3.90 (sept, 4H, *o-i*Pr-CH, $^{3}J_{HH} = 6.6$ Hz), 4.35 (pseudo-t, 4H), 4.37 (pseudo-t, 4H), 4.50 (s, 10H, Cp), 7.25 (s, 4H, Ar-H); $^{13}$C NMR (75 MHz, rt, $C_6D_6$): $\delta$ 24.77 (q), 25.72 (q), 25.57 (q), 35.14 (d), 34.91 (d), 67.31 (s), 67.97 (d), 69.87 (d), 72.24 (d), 121.10 (d), 128.84 (s), 151.73 (s), 156.24 (s); $^{29}$Si NMR (59 MHz, rt, $C_6D_6$): $\delta$ 12.4. HRMS (FAB) *m/z* Calcd for $C_{50}H_{65}O_2{}^{102}Ru_2Si_2$ 956.2532 $[M + H]^+$. Found 956.2564 $[M + H]^+$.

**Reaction of (*E*)-1,2-Bis(ferrocenyl)-1,2-bis(2,4,6-triisopropylphenyl)disilene (1a) with $S_8$.** To a benzene solution (15 mL) of **1a** (50.0 mg, 60.0 µmol) was added $S_8$ (9.6 mg, 37.5 µmol, 5 equiv as S) at room temperature and the solution turned orange. The solution was then filtered with Celite® to remove excess $S_8$. After removal of the solvent of the filtration, the reaction mixture was separated by GPLC to afford the corresponding thiadisilirane, Tip(Fc)Si($\mu$-S)Si(Fc)Tip (**6**, 42.0 mg, 48.6 µmol 81%) and 1,2,3,4-dithiadisiletane, Tip(Fc)Si($\mu$-$S_2$)Si-(Fc)Tip (**7**, 7.25 mg, 8.09 µmol 13%). **6**; orange crystals; mp 181.2–183.0 °C; $^{1}$H NMR (300 MHz, rt, $C_6D_6$): $\delta$ 1.18 (d, 6H, *p-i*Pr-Me, $^{3}J_{HH} = 6.6$ Hz), 1.20 (d, 6H, *p-i*Pr-Me, $^{3}J_{HH} = 6.6$ Hz), 1.23 (d, 6H, *o-i*Pr-Me, $^{3}J_{HH} = 6.6$ Hz), 1.25 (d, 6H, *o-i*Pr-Me, $^{3}J_{HH} = 6.6$ Hz), 1.62 (d, 6H, *o-i*Pr-Me, $^{3}J_{HH} = 6.6$ Hz), 1.84 (d, 6H, *o-i*Pr-Me, $^{3}J_{HH} = 6.6$ Hz), 2.83 (sept, 2H, *o-i*Pr-CH, $^{3}J_{HH} = 6.6$ Hz), 3.71 (sept, 2H, *p-i*Pr-CH, $^{3}J_{HH} = 6.6$ Hz), 3.72 (m, 2H, Cp), 3.84 (m, 2H, Cp), 3.91 (m, 2H, Cp), 3.94 (m, 2H, Cp), 4.24 (s, 10H, Cp), 4.68 (sept, 2H, *o-i*Pr-CH, $^{3}J_{HH} = 6.6$ Hz), 7.13 (d, 2H, Ar-H, $^{4}J_{HH} = 1.8$ Hz), 7.34 (d, 2H, Ar-H, $^{4}J_{HH} = 1.8$ Hz); $^{13}$C NMR (75 MHz, rt, $C_6D_6$): $\delta$ 24.06 (q), 24.07 (q), 24.50 (q), 25.30 (q), 25.85 (q), 26.25 (q), 34.70 (d), 36.17 (d), 37.12 (d), 68.85 (d), 69.29 (s), 70.66 (d), 71.70 (d), 73.13 (d), 76.83 (d), 122.09 (d), 122.42 (d), 128.12 (s), 151.64 (s), 155.61 (s), 156.95 (s); $^{29}$Si NMR (59 MHz, rt, $C_6D_6$): $\delta$ −50.8. HRMS (FAB) *m/z* Calcd for $C_{50}H_{64}{}^{56}Fe_2Si_2{}^{32}S$ 864.2966 $[M]^+$. Found 864.2926 $[M]^+$. Anal. Calcd for $C_{50}H_{64}Fe_2Si_2S$: C, 69.43; H, 7.46; S, 3.71%. Found: C, 69.22; H, 7.73; S, 3.53%. **7**; orange crystals; mp 193.4–195.7 °C; $^{1}$H NMR (300 MHz, rt, $C_6D_6$): $\delta$ 0.91 (d, 6H, *p-i*Pr-Me, $^{3}J_{HH} = 6.6$ Hz), 1.18 (d, 6H, *p-i*Pr-Me, $^{3}J_{HH} = 6.6$ Hz), 1.28 (d, 6H, *o-i*Pr-Me, $^{3}J_{HH} = 6.6$ Hz), 1.29 (d, 6H, *o-i*Pr-Me, $^{3}J_{HH} = 6.6$ Hz), 1.53 (d, 6H, *o-i*Pr-Me, $^{3}J_{HH} = 6.6$ Hz), 1.94 (d, 6H, *o-i*Pr-Me, $^{3}J_{HH} = 6.6$ Hz), 2.87 (sept, 2H, *o-i*Pr-CH, $^{3}J_{HH} = 6.6$ Hz), 2.98 (sept, 2H, *p-i*Pr-CH, $^{3}J_{HH} = 6.6$ Hz), 3.98 (m, 2H, Cp), 3.99 (m, 2H, Cp), 4.00 (m, 2H, Cp), 4.03 (m, 2H, Cp), 4.11 (s, 10H, Cp), 4.81 (sept, 2H, *o-i*Pr-CH, $^{3}J_{HH} = 6.6$ Hz), 7.10 (d, 2H, Ar-H, $^{4}J_{HH} = 1.2$ Hz), 7.41 (d, 2H, Ar-H, $^{4}J_{HH} = 1.2$ Hz); $^{13}$C NMR (75 MHz, rt, $C_6D_6$): $\delta$ 24.03 (q), 24.11 (q), 24.51 (q), 26.22 (q), 26.40 (q), 27.76 (q), 32.99 (d), 34.56 (d), 35.81 (d), 68.88 (d), 70.51 (d), 71.94 (d), 73.82 (s), 74.82 (d), 76.66 (d), 121.47 (d), 122.97 (d), 125.04 (s), 151.09 (s), 151.21 (s), 156.48 (s); $^{29}$Si NMR (59 MHz, rt, $C_6D_6$): $\delta$ 25.5. HRMS (FAB) *m/z* Calcd for $C_{50}H_{64}{}^{56}Fe_2Si_2{}^{32}S_2$ 896.2687 $[M]^+$. Found 896.2690 $[M]^+$. Anal. Calcd for $C_{50}H_{64}Fe_2Si_2S_2$: C, 66.95; H, 7.19%. Found: C, 66.63; H, 6.89%.

**Reaction of (*E*)-1,2-Bis(ferrocenyl)-1,2-bis(2,4,6-triisopropylphenyl)disilene (1a) with Elemental Se.** To a benzene solution (10 mL) of **1a** (20.0 mg, 24.0 µmol) was added elemental selenium (grey Se, 18.9 mg, 0.240 mmol, 10 equiv) at room temperature and the solution turned orange. The solution was then filtered with Celite® to remove excess Se. After the removal of solvent, the reaction mixture was separated by GPLC to the afford corresponding selenadisilirane, Tip(Fc)Si($\mu$-Se)Si(Fc)Tip (**9**, 20.7 mg, 22.7 µmol, 95%). **9**; orange crystals; mp 171.6–172.4 °C; $^{1}$H NMR (300 MHz, rt, $C_6D_6$): $\delta$ 1.15 (d, 6H, *o-i*Pr-Me, $^{3}J_{HH} = 6.6$ Hz), 1.19 (d, 6H, *o-i*Pr-Me, $^{3}J_{HH} = 6.6$ Hz), 1.24 (d, 6H, *o-i*Pr-Me, $^{3}J_{HH} = 6.6$ Hz), 1.25 (d, 6H, *o-i*Pr-Me, $^{3}J_{HH} = 6.6$ Hz), 1.61 (d, 6H, *p-i*Pr-Me, $^{3}J_{HH} = 6.6$ Hz), 1.84 (d, 6H, *p-i*Pr-Me, $^{3}J_{HH} = 6.6$ Hz), 2.83 (sept, 2H, *o-i*Pr-CH, $^{3}J_{HH} = 6.6$ Hz), 3.69 (sept, 2H, *o-i*Pr-CH, $^{3}J_{HH} = 6.6$ Hz), 3.75 (m, 2H, Cp), 3.86 (m, 2H, Cp), 3.93 (m, 2H, Cp), 3.98 (m, 2H, Cp), 4.20 (s, 10H, Cp), 4.81 (sept, 2H, *p-i*Pr-CH, $^{3}J_{HH} = 6.6$ Hz), 7.16 (d, 2H, Ar-H, $^{4}J_{HH} = 1.2$ Hz), 7.34 (d, 2H, Ar-H, $^{4}J_{HH} = 1.2$ Hz); $^{13}$C NMR (75 MHz, rt, $C_6D_6$): $\delta$ 24.04 (q), 24.07 (q), 24.27 (q), 25.57 (q), 26.09 (q), 26.50 (q), 34.66 (d), 36.38 (d), 37.41 (d), 68.49 (d), 69.05 (s), 70.60 (d), 71.48 (d), 73.26 (d), 76.99 (d), 121.06 (d), 122.68 (d), 127.32 (s), 151.60 (s), 155.51 (s), 157.26 (s); $^{29}$Si NMR (59 MHz, rt, $C_6D_6$): $\delta$ −56.4 (s, $^{1}J_{SiSe} = 77$ Hz); $^{77}$Se NMR (76 MHz, rt, $C_6D_6$): $\delta$ −309.8 (s, $^{1}J_{SiSe} = 77$ Hz). HRMS (FAB) *m/z* Calcd for $C_{50}H_{64}{}^{56}Fe_2{}^{80}SeSi_2$ 912.2421 $[M]^+$. Found 912.2408 $[M]^+$. Anal. Calcd for $C_{50}H_{64}Fe_2SeSi_2 + C_7H_8$: C, 68.19; H, 7.23%. Found: C, 68.40; H, 7.36%.

**Heating 7 in Toluene Solution.** A toluene-*d*$_8$ solution (4 mL) of **7** (5.0 mg, 5.6 µmol) in a sealed tube was heated at 140 °C for 20 h. No change was observed as judged by $^{1}$H NMR spectra.

**Attempted Sulfurization of 6 in Benzene Solution.** To a benzene-*d*$_6$ solution (4 mL) of **6** (5.0 mg, 5.6 µmol) was added $S_8$ (2.2 mg, 7.0 µmol, 10 equiv as S) and $NEt_3$ (1.8 mg, 7.0 µmol, 10 equiv as S) in a sealed tube. The sealed tube was then heated at 80 °C for 1 h. No change was observed as judged by $^{1}$H NMR spectra.

**Attempted Desulfurization of 7 in Benzene Solution.** To a benzene-*d*$_6$ solution (4 mL) of **7** (5.0 mg, 5.8 µmol) was added excess $PPh_3$ (14.6 mg, 55.7 µmol, 10 equiv) in a sealed tube. The sealed tube was then heated at 80 °C for 1 h. No change was observed as judged by $^{1}$H NMR spectra.

**Attempted Deselenization of 9 in a Benzene Solution.** To a benzene-*d*$_6$ solution (4 mL) of **9** (5.0 mg, 5.5 µmol) was added excess $PPh_3$ (14.4 mg, 54.8 µmol, 10 equiv) in a sealed tube. The sealed tube was then heated at 60 °C for 3 days or light irradiated with a medium pressure mercury lamp for 1 h through Pyrex® glass. No change was observed as judged by $^{1}$H NMR spectra.

**X-ray Crystallographic Analyses of 1a, 1b, 2a, 2b, 5a, 5b, 6, 7, and 9.** The intensity data were collected on a Rigaku/MSC Mercury CCD diffractometer with graphite monochromated

**Table 5.** Crystal Data of **1a**–**2b**, **5a**–**7**, and **9**

|  | **1a**[13] | **1b** | **2a**[13] | **2b** | **5a**[35] | **5b** | **6** | **7** | **9**[35] |
|---|---|---|---|---|---|---|---|---|---|
| Empirical formula | $C_{50}H_{64}Fe_2Si_2\cdot C_4H_8O$ | $C_{50}H_{64}Ru_2Si_2$ | $C_{25}H_{32}Cl_2FeSi\cdot 1.5\cdot C_6H_6$ | $C_{25}H_{32}Cl_2RuSi$ | $C_{50}H_{64}O_2Fe_2Si_2$ | $C_{50}H_{64}O_2Ru_2Si_2$ | $C_{50}H_{64}Fe_2Si_2S\cdot 0.5\cdot C_6H_{14}$ | $C_{50}H_{64}Fe_2Si_2S_2$ | $C_{50}H_{64}Fe_2SeSi_2\cdot C_7H_8$ |
| Formula weight | 904.99 | 923.33 | 601.51 | 532.57 | 864.89 | 955.33 | 908.04 | 897.01 | 1003.99 |
| Temperature/K | 103(3) | 103(3) | 103(3) | 103(2) | 103(3) | 103(2) | 103(2) | 103(2) | 103(2) |
| Crystal size/mm$^3$ | 0.45 × 0.40 × 0.10 | 0.08 × 0.03 × 0.01 | 0.80 × 0.70 × 0.50 | 0.20 × 0.15 × 0.01 | 0.08 × 0.02 × 0.01 | 0.20 × 0.15 × 0.01 | 0.12 × 0.05 × 0.01 | 0.05 × 0.02 × 0.01 | 0.20 × 0.10 × 0.01 |
| Crystal system | monoclinic | trigonal | triclinic | monoclinic | triclinic | triclinic | monoclinic | tetragonal | triclinic |
| Space group | $C2/c$ (#15) | $R\bar{3}$ (#148) | $P\bar{1}$ (#2) | $P2_1/c$ (#14) | $P\bar{1}$ (#2) | $P\bar{1}$ (#2) | $P2_1/n$ (#14) | $I4_1/a$ (#88) | $P\bar{1}$ (#2) |
| $a$/Å | 19.3619(7) | 30.7254(3) | 9.2133(4) | 14.8280(5) | 10.2128(2) | 9.8074(6) | 15.8824(3) | 41.3616(7) | 13.0831(3) |
| $b$/Å | 10.0596(3) | 30.7258(3) | 12.524(5) | 6.0179(2) | 10.5104(3) | 10.6147(6) | 17.0262(3) | 41.3616(7) | 13.3764(4) |
| $c$/Å | 260871(8) | 14.9090(2) | 15.1047(5) | 27.1506(10) | 11.1103(3) | 12.9198(10) | 18.2170(4) | 10.8338(2) | 17.6020(4) |
| $\alpha$/deg | 90 | 90 | 70.818(19) | 90 | 94.4274(12) | 70.879(4) | 90 | 90 | 107.3655(10) |
| $\beta$/deg | 106.2743(13) | 90 | 80.00(2) | 91.5905(16) | 109.8355(12) | 72.729(3) | 98.6825(10) | 90 | 98.6234(11) |
| $\gamma$/deg | 90 | 120 | 69.201(15) | 90 | 94.5322(17) | 71.058(3) | 90 | 90 | 114.8772(18) |
| $V$/Å$^3$ | 4877.5(3) | 12189.2(2) | 1535.60(8) | 2421.81(15) | 1111.42(5) | 1174.32(16) | 4869.73(17) | 18534.3(6) | 2525.61(11) |
| $Z$ value | 4 | 9 | 2 | 4 | 1 | 1 | 4 | 16 | 2 |
| $D_{calcd}$/g cm$^{-3}$ | 1.232 | 1.132 | 1.307 | 1.461 | 1.292 | 1.351 | 1.239 | 1.286 | 1.377 |
| No. of reflections (all) | 4530 | 4731 | 4744 | 4249 | 4111 | 4120 | 9064 | 8624 | 9349 |
| No. of parameters | 273 | 250 | 350 | 262 | 259 | 259 | 536 | 517 | 572 |
| No. of restraints | 0 | 0 | 0 | 0 | 0 | 0 | 0 | 0 | 0 |
| $R_1$ ($I > 2\sigma(I)$) | 0.0446 | 0.0281 | 0.0672 | 0.0503 | 0.0291 | 0.0485 | 0.0539 | 0.0460 | 0.0388 |
| $wR_2$ (all data) | 0.1238 | 0.0747 | 0.1757 | 0.1015 | 0.0681 | 0.1167 | 0.1225 | 0.0921 | 0.0682 |
| Goodness of fit | 1.066 | 1.087 | 1.132 | 1.046 | 1.075 | 1.014 | 1.020 | 1.013 | 1.010 |

Mo K$\alpha$ radiation ($\lambda = 0.71070$ Å) for **1a**, **2a**, and **5b** and on a RIGAKU Saturn70 CCD(system) with VariMax Mo Optic using Mo K$\alpha$ radiation ($\lambda = 0.71070$ Å) for **1b**, **2b**, **5a**, **6**, **7**, and **9**. Single crystals suitable for X-ray analysis were obtained by slow recrystallization from THF (for **1a** and **1b**), benzene (for **2a** and **2b**), hexane (for **5a**, **5b**, **6**, and **7**), and toluene (for **9**) at room temperature (Figures 3, 4, 6, 7, and 15–19 and Table 5). Each crystal was mounted on a glass fiber. The structures were solved by direct method (SIR-97[36]) and refined by full-matrix least-squares procedures on $F^2$ for all reflections (SHELXL-97[37]). All hydrogen atoms were placed using AFIX instructions, while all other atoms were refined anisotropically. Crystallographic data (excluding structure factors) for the structure reported in this paper have been deposited with the Cambridge Crystallographic Data Centre as supplementary publication nos. CCDC 701201 for **1a**,[13] CCDC 712630 for **1b**, CCDC 701202 for **2a**,[13] CCDC 712631 for **2b**, CCDC 699677 for **5a**,[38] CCDC 712632 for **5b**, CCDC 712633 for **6**, CCDC 712634 for **7**, and CCDC 699678 for **9**.[38] Copies of the data can be obtained free of charge on application to CCDC, 12, Union Road, Cambridge, CB2 1EZ, U.K. (fax: +44 1223 336033; E-mail: deposit@ccdc.cam.ac.uk).

This work was partially supported by Grants-in-Aid for Creative Scientific Research (No. 17GS0207), Science Research on Priority Areas (Nos. 19027024 and 20036024 "Synergy of Elements"), and the Global COE Program ("Integrated Materials Science"), Kyoto University from Ministry of Education, Culture, Sports, Science and Technology, Japan.

## References

1 For example, see: a) K. Tanaka, K. Ohzeki, S. Nankai, T. Yamabe, H. Shirakawa, *J. Phys. Chem. Solids* **1983**, *44*, 1069. b) J. Jacob, J. Zhang, A. C. Grimsdale, K. Müllen, M. Gaal, E. J. W. List, *Macromolecules* **2003**, *36*, 8240. c) J. Jacob, S. Sax, T. Piok, E. J. W. List, A. C. Grimsdale, K. Müllen, *J. Am. Chem. Soc.* **2004**, *126*, 6987. d) C. Xia, R. C. Advincula, *Macromolecules* **2001**, *34*, 6922. e) S. Qiu, P. Lu, X. Liu, F. Shen, L. Liu, Y. Ma, J. Shen, *Macromolecules* **2003**, *36*, 9823. f) C. Former, S. Becker, A. C. Grimsdale, K. Müllen, *Macromolecules* **2002**, *35*, 1576. g) S. A. Jenekhe, A. Babel, *J. Am. Chem. Soc.* **2003**, *123*, 13656. h) S. Yamaguchi, C. Xu, T. Okamoto, *Pure Appl. Chem.* **2006**, *78*, 721.

2 a) *Ferrocenes,* ed. by A. Togni, T. Hayashi, VCH, Weinheim, Germany, **1995**, and references cited therein. b) Y. Yamaguchi, W. Ding, C. T. Sanderson, M. L. Borden, M. J. Morgan, C. Kutal, *Coord. Chem. Rev.* **2007**, *251*, 515.

3 For recent reviews, see: a) W. Kaim, G. K. Lahiri, *Angew. Chem., Int. Ed.* **2007**, *46*, 1778. b) M. Kurihara, H. Nishihara, *Coord. Chem. Rev.* **2002**, *226*, 125. c) K. D. Demadis, C. M. Hartshorn, T. Meyer, *Chem. Rev.* **2001**, *101*, 2655. d) A. J. Distefano, J. F. Wishart, S. S. Isied, *Coord. Chem. Rev.* **2005**, *249*, 507. e) S. Szafert, J. A. Gladysz, *Chem. Rev.* **2006**, *106*, PR1.

4 For example, see: a) W. Kaim, G. K. Lahiri, *Angew. Chem., Int. Ed.* **2007**, *46*, 1778. b) D. M. D'Alessandro, F. R. Keene, *Chem. Rev.* **2006**, *106*, 2270.

5 a) W. Skibar, H. Kopacka, K. Wurst, C. Salzmann, K. H. Ongania, F. F. de Biani, P. Zanello, B. Bildstein, *Organometallics* **2004**, *23*, 1024. b) B. Bildstein, A. Hradsky, H. Kopacka, R. Malleier, K. H. Ongania, *J. Organomet. Chem.* **1997**, *540*, 127. c) A. Hradsky, B. Bildstein, N. Schuler, H. Schottenberger, P. Jaitner, K. H. Ongania, K. Wurst, J. P. Launay, *Organometallics*

**1997**, *16*, 392.

6 a) M. Kurosawa, T. Nankawa, T. Matsuda, K. Kubo, M. Kurihara, H. Nishihara, *Inorg. Chem.* **1999**, *38*, 5113. b) M. Kurihara, T. Matsuda, A. Hirooka, T. Yutaka, H. Nishihara, *J. Am. Chem. Soc.* **2000**, *122*, 12373. c) H. Nishihara, *Coord. Chem. Rev.* **2005**, *249*, 1468.

7 a) N. Nagahora, T. Sasamori, N. Takeda, N. Tokitoh, *Chem.—Eur. J.* **2004**, *10*, 6146. b) N. Nagahora, T. Sasamori, N. Tokitoh, *Chem. Lett.* **2006**, *35*, 220. c) N. Nagahora, T. Sasamori, Y. Watanabe, Y. Furukawa, N. Tokitoh, *Bull. Chem. Soc. Jpn.* **2007**, *80*, 1884. d) C. Moser, M. Nieger, R. Pietschnig, *Organometallics* **2006**, *25*, 2667. e) C. Moser, A. Orthaber, M. Nieger, F. Belaj, R. Pietschnig, *Dalton Trans.* **2006**, 3879.

8 R. West, M. J. Fink, J. Michl, *Science* **1981**, *214*, 1343.

9 For reviews, see: a) R. Okazaki, R. West, *Adv. Organomet. Chem.* **1996**, *39*, 231. b) M. Weidenbruch, in *The Chemistry of Organic Silicon Compounds,* ed. by Z. Rappoport, Y. Apeloig, John Wiley & Sons, Chichester, U.K., **2001**, Vol. 3, p. 391. c) R. West, *Polyhedron* **2002**, *21*, 467. d) M. Kira, T. Iwamoto, *Adv. Organomet. Chem.* **2006**, *54*, 73. e) T. Sasamori, N. Tokitoh, in *Encyclopedia of Inorganic Chemistry*, 2nd ed., ed. by R. B. King, Wiley Chichester, U.K., **2005**, p. 1698.

10 For example, see: a) A. G. Brook, F. Abdesaken, B. Gutekunst, G. Gutekunst, R. K. Kallury, *J. Chem. Soc., Chem. Commun.* **1981**, 191. b) H. Ottosson, A. M. Eklöf, *Coord. Chem. Rev.* **2008**, *252*, 1287.

11 a) N. Wiberg, W. Niedermayer, G. Fischer, H. Nöth, M. Suter, *Eur. J. Inorg. Chem.* **2002**, 1066. b) A. Sekiguchi, R. Kinjo, M. Ichinohe, *Science* **2004**, *305*, 1755. c) A. Sekiguchi, M. Ichinohe, R. Kinjo, *Bull. Chem. Soc. Jpn.* **2006**, *79*, 825. d) A. Sekiguchi, *Pure Appl. Chem.* **2008**, *80*, 447. e) T. Sasamori, K. Hironaka, Y. Sugiyama, N. Takagi, S. Nagase, Y. Hosoi, Y. Furukawa, N. Tokitoh, *J. Am. Chem. Soc.* **2008**, *130*, 13856.

12 a) I. Bejan, D. Scheschkewitz, *Angew. Chem., Int. Ed.* **2007**, *46*, 5783. b) A. Fukazawa, Y. Li, S. Yamaguchi, H. Tsuji, K. Tamao, *J. Am. Chem. Soc.* **2007**, *129*, 14164.

13 T. Sasamori, A. Yuasa, Y. Hosoi, Y. Furukawa, N. Tokitoh, *Organometallics* **2008**, *27*, 3325.

14 a) M. G. Hill, W. M. Lamanna, K. R. Mann, *Inorg. Chem.* **1991**, *30*, 4687. b) S. Trupia, A. Nafady, W. E. Geiger, *Inorg. Chem.* **2003**, *42*, 5480. c) Reversibility of the cyclic voltammogram of ruthenocene depends on the conditions. For example, see: R. J. Gale, R. Job, *Inorg. Chem.* **1981**, *20*, 42.

15 I. R. Butler, S. B. Wilkes, S. J. McDonald, L. J. Hobson, A. Taralp, C. P. Wilde, *Polyhedron* **1993**, *12*, 129.

16 C. N. Smit, F. Bickelhaupt, *Organometallics* **1987**, *6*, 1156.

17 Trans-bent angle for the disilene is defined as the angle between the R–Si–R plane and Si–Si axis.

18 B3PW91/6-31+G(2d)[6-31G(d) for C, H, DZVP for Fe, Ru].

19 N. Godbout, D. R. Salahub, J. Andzelm, E. Wimmer, *Can. J. Chem.* **1992**, *70*, 560.

20 L. A. Leites, S. S. Bukalov, J. E. Mangette, T. A. Schmedake, R. West, *Spectrochim. Acta, Part A* **2003**, *59*, 1975.

21 a) B. D. Shepherd, R. West, *Chem. Lett.* **1988**, 183. b) M. Kira, T. Ishima, T. Iwamoto, M. Ichinohe, *J. Am. Chem. Soc.* **2001**, *123*, 1676.

22 M. Sato, Y. Kawata, A. Kudo, A. Iwai, H. Saitoh, S. Ochiai, *J. Chem. Soc., Dalton Trans.* **1998**, 2215.

23 a) M. J. Michalczyk, R. West, J. Michl, *J. Chem. Soc., Chem. Commun.* **1984**, 1525. b) M. J. Michalczyk, M. J. Fink, K. J. Haller, R. West, J. Michl, *Organometallics* **1986**, *5*, 531. c) B. D. Shepherd, D. R. Powell, R. West, *Organometallics* **1989**, *8*, 2664. d) A. J. Millevolte, D. R. Powell, S. G. Johnson, R. West, *Organometallics* **1992**, *11*, 1091. e) K. L. McKillop, G. R. Gillette, D. R. Powell, R. West, *J. Am. Chem. Soc.* **1992**, *114*, 5203.

24 a) R. West, D. J. D. Young, K. J. Haller, *J. Am. Chem. Soc.* **1985**, *107*, 4942. b) J. E. Mangette, D. R. Powell, R. West, *Organometallics* **1995**, *14*, 3551.

25 R. P. Tan, G. R. Gillette, D. R. Powell, R. West, *Organometallics* **1991**, *10*, 546.

26 N. Wiberg, W. Niedermayer, K. Polborn, P. Mayer, *Chem.—Eur. J.* **2002**, *8*, 2730.

27 Yoshifuji and his co-workers have already reported that the reactions of Mes$^*$P=PMes$^*$ with $S_8$ in $NEt_3$ resulted in the formation of the corresponding thiadiphosphirane derivative, Mes$^*$P(S)PMes$^*$ (Mes$^*$ = 2,4,6-tri-*t*-buthylphenyl).

28 a) V. Y. Lee, S. Miyazaki, H. Yasuda, A. Sekiguchi, *J. Am. Chem. Soc.* **2008**, *130*, 2758. b) H. Suzuki, N. Tokitoh, R. Okazaki, *Bull. Chem. Soc. Jpn.* **1995**, *68*, 2471.

29 a) M. Yoshifuji, K. Shibayama, N. Inamoto, *Chem. Lett.* **1984**, 603. b) N. Nakata, N. Takeda, N. Tokitoh, *Chem. Lett.* **2002**, 818.

30 B3PW91/6-311+G(3d)[6-31G(d) for C, H, DZVP for Fe, Ru].

31 A. Schäfer, M. Weidenbruch, W. Saak, S. Pohl, H. Marsmann, *Angew. Chem., Int. Ed. Engl.* **1991**, *30*, 962.

32 W. S. Sheldrick, in *The Chemistry of Organic Silicon Compounds*, ed. by S. Patai, Z. Rappoport, John Wiley & Sons, Chichester, New York, **1989**, Part 1, p. 249.

33 T. Kudo, S. Akiba, Y. Kondo, H. Watanabe, K. Morokuma, T. Vreven, *Organometallics* **2003**, *22*, 4721.

34 A. B. Pangborn, M. A. Giardello, R. H. Grubbs, R. K. Rosen, F. J. Timmers, *Organometallics* **1996**, *15*, 1518.

35 M. J. Frisch, G. W. Trucks, H. B. Schlegel, G. E. Scuseria, M. A. Robb, J. R. Cheeseman, J. A. Montgomery, T. Vreven, K. N. Kudin, J. C. Burant, J. M. Millam, S. S. Iyengar, J. Tomasi, V. Barone, B. Mennucci, M. Cossi, G. Scalmani, N. Rega, G. A. Petersson, H. Nakatsuji, M. Hada, M. Ehara, K. Toyota, R. Fukuda, J. Hasegawa, M. Ishida, T. Nakajima, Y. Honda, O. Kitao, H. Nakai, M. Klene, X. Li, J. E. Knox, H. P. Hratchian, J. B. Cross, V. Bakken, C. Adamo, J. Jaramillo, R. Gomperts, R. Stratmann, E. E. Yazyev, A. J. Austin, R. Cammi, C. Pomelli, J. W. Ochterski, P. Y. Ayala, K. Morokuma, G. A. Voth, P. Salvador, J. J. Dannenberg, V. G. Zakrzewski, S. Dapprich, A. D. Daniels, M. C. Strain, O. Farkas, D. K. Malick, A. D. Rabuck, K. Raghavachari, J. B. Foresman, J. V. Ortiz, Q. Cui, A. G. Baboul, S. Clifford, J. Cioslowski, B. B. Stefanov, G. Liu, A. Liashenko, P. Piskorz, L. Komaromi, R. L. Martin, D. J. Fox, T. Keith, M. A. Al-Laham, C. Y. Peng, A. Nanayakkara, M. Challacombe, P. M. W. Gill, B. Johnson, W. Chen, M. W. Wong, C. Gonzalez, J. A. Pople, *Gaussian 03, Revision E.01*, Gaussian, Inc., Wallingford CT, **2004**.

36 A. Altomare, M. Burla, M. Camalli, G. Cascarano, C. Giacovazzo, A. Guagliardi, A. Moliterni, G. Polidori, R. Spagna, *J. Appl. Crystallogr.* **1999**, *32*, 115.

37 a) G. M. Sheldrick, *Acta Crystallogr., Sect. A* **1990**, *46*, 467. b) G. Sheldrick, *SHELX-97, Program for Crystal Structure Solution and the Refinement of Crystal Structures*, Institüt für Anorganische Chemie der Universität Göttingen, Tammanstrasse 4, D-3400 Göttingen, Germany, 1997.

38 N. Tokitoh, A. Yuasa, T. Sasamori, *Phosphorus, Sulfur Silicon*, in press.